

UNIQUE PRESSURE- AND RATE-DEPENDENT ADHESION CAPABILITIES OF POLLENS

J. Carson Meredith, Haisheng Lin, Donglee Shin and Zihao Qu

School of Chemical & Biomolecular Engineering, Georgia Institute of Technology

Natural particles, such as pollen, diatoms, and fungal spores, exhibit a remarkable breadth of complex solid surface ornamentations as well as thin liquid glues. This talk will examine plant pollen microparticles, and illustrate their unique load- and rate-dependent adhesion mechanisms. The size, arrangement and shape of solid spines on sunflower and ragweed pollen allow a load-dependent adhesion with their natural stigma ‘mating’ surfaces. This structural-based driven load-dependent behavior is based on alignment of spines on the pollen with complementary-spaced features on the stigma. The load-dependent behavior can be mimicked with patterned synthetic polymers, such as styrene-isoprene copolymers. Pollen also can tune their adhesion to surfaces through its viscous two-phase oil-water pollenkitt fluid coating. Pollenkitt fluid forms nanoscale capillary bridges that are very sensitive to both the dynamics (speed) of detachment and to the presence of surface patterns.

Introduction

It is well known that adhesion of solid surfaces can be affected greatly by both the presence of solid surface asperities or undulations and by the presence of wetting liquids.¹ In addition, the presence of solid-solid contact can be complex and induce large changes to adhesion if the surface patterns are complementary and ‘match’ in some characteristic length or shape parameter. When wet adhesion is controlled by static equilibrium capillary forces alone, the adhesion is not dependent on separation rate. However, as the viscosity and shear rate increase, hydrodynamic contributions can begin to dominate the liquid bridges, leading to rate dependent behavior.

Adhesion by liquid bridges is important for wet adhesion in Nature, including pollens,² spiders,³ insects,⁴ tree frogs,⁵ and geckos.⁶ It is also very important for applications involving granular materials, particles (e.g., hard disk drives, dust filters), nanolithography, and adhesives. In Nature, many of the surfaces spanned by liquid bridges have complex geometries, such as spiky, hairy, fibrillar and other hierarchically-structured surfaces. However, knowledge of the wet adhesive mechanisms of viscous liquid bridges between surfaces with such complex geometries is quite limited.

An important, but overlooked example of these is pollen. Pollens are well-known micro particles with organized fine-scale surface morphology (Figure 1),² and pollenkitt is a liquid adhesive material coating the surface of many pollens, especially those pollinated by animals.⁷ Pollenkitt liquid coatings form capillary bridges that are significant in dictating the magnitude and humidity dependence of pollen adhesion forces. In addition to the spiny features of pollens, many flower stigma surfaces, the natural ‘mating’ surface of a pollen, consist of pattered micron-sized papillae. These features suggest that pollen and stigma may demonstrate physical specificity through pattern interlocking. Pollen adhesion is critical to the complex steps in pollen transport in which multiple detachment and reattachment steps occur. For example, the pollens

of plants pollinated by animals must (i) be easily removed from one flower by the pollinator, (ii) adhere well to the pollinator during transport, and (iii) readily release onto a complementary plant stigma surface. How pollen and stigma surfaces utilize capillary, hydrodynamic, and complimentary surface patterns to accomplish such feats is not well understood. Thus, we have undertaken studies to better understand the quantitative features of pollen adhesion, specifically the role of surface patterning and liquid bridges.

By using pollen and stigma as a model, we report the first observation of pressure-dependent adhesion of a single microparticle mediated by complementary physical structures. This load-sensitive particle adhesion is mediated by the interlocking patterns on the surfaces of pollen and stigma from the same botanical family. Inspired by this result, we showed that this loading-dependent adhesion can be replicated with blends of polystyrene (PS) with a triblock copolymer: polystyrene-*b*-polyisoprene-*b*-polystyrene (PSI). We also report that viscous liquid pollenkitt bridges result in a remarkable dynamic rate-dependent wet adhesion, which can be adjusted rationally by tuning the size of the spiny features on the pollen particle surface. The magnitude and hydrodynamic response of the wet adhesion due to the shear thinning viscous liquid bridge were modeled by combining expressions for the static capillary and dynamic viscous forces. The length of pollen spines is found to control whether the liquid bridges form around a single spine or multiple spines, allowing tuning of the magnitude and dynamic range of viscous forces. Mimicry of these features may offer inspiration for new adhesion mechanisms for microparticles, particularly those that are responsive to the dynamics of particle detachment speed.

Materials and Methods

Pollen and Stigma Preparation. Native non-defatted grains of ragweed (*Ambrosia artemisiifolia*) and sunflower (*Helianthus annuus*) pollens were purchased from Greer Laboratories (Lenoir, NC). A non-echinate variety, olive (*Olea europaea*, Po), was chosen as a control. The pollen grains were immersed in a chloroform and methanol mixture (3:1) for 24 h, in order to extract pollenkitt. Other details of cleaning and preparation procedures are given in previous publications.⁸⁻¹⁰ Pollens denoted as “cleaned” below were prepared in this way, (shown in Figure 1), and pollens used without cleaning were denoted as “native”. The separation and collection of pollenkitt were accomplished by a chloroform and methanol mixture (3:1) solvent extraction from dandelion (*Taraxacum officinale*) as described in a previous study.⁹

Force measurements. Adhesion of pollens was measured using atomic force microscopy (AFM, Veeco Dimension 3100) at different separation rates (from 500 to 67000 nm/s). The AFM cantilever was located 6 μm above the silicon support prior to approach and the same approach rate of 500 nm/s was used for all experiments, even those in which separation rate was varied. Holding the initial approach velocity constant allows for a consistent particle contact with the pollenkitt films as well as an initial volume of liquid wetting the particles. Tipless rectangular cantilevers (Fort-TL, AppNano Inc., Santa Clara, CA) with nominal spring constants of 0.6~3.7 N/m were used to fabricate colloidal probes consisting of a single pollen grain attached by a small amount of epoxy resin (Epoxy Marine, Loctite, Westlake, OH).⁸⁻¹⁰

Fabrication of Stigma Mimicking Patterned Polymer Surfaces. Polystyrene with three different molecular masses (PS1, $M_w = 1.3$ kDal with $M_w/M_n = 1.06$; PS2, $M_w = 13$ kDal with

$M_w/M_n = 1.06$; PS3, $M_w = 230$ kDal with $M_w/M_n = 1.64$; Sigma-Aldrich) and polystyrene-block-polyisoprene-block-polystyrene (PSI, 17 % by mass styrene, $M_n = 1.9$ kDal, Sigma-Aldrich) were used as received. To generate conical-patterned surfaces with PS1, PS2 and PS3 blended with PSI, the mass ratio of PS:PSI was kept at 1:4, and the roughness of the phase-separated pattern was varied by adjusting the PS chain length. Pure PS3 was used as a control smooth surface, hereafter referred to simply as PS. The PS and the blend solutions were prepared by dissolving 10% by mass of the following polymers in toluene: PS = 10% PS3; PS1I = 2% PS1 + 8% PSI; PS12 = 2% PS2 + 8% PSI; PS13 = 2% PS3 + 8% PSI.¹⁰

Scanning Electron Microscopy (SEM). The surface morphology of the pollen grains was characterized by scanning electron microscopy (SEM) (Zeiss Ultra60 FE-SEM, Zeiss, Germany) at accelerating the potential of 5.0 kV. Cleaned defatted pollens were sputtered with gold and then mounted on metal stubs using carbon tape.

Viscosity Measurement. The viscosity of the pollenkitt solution was measured with a rotational rheometer (PHYSICA MCR 300, Anton Paar) in a cone and plate geometry with a plate diameter of 25 mm. The measurement was performed over a range of shear rate from 1~100 s⁻¹ at room temperature.

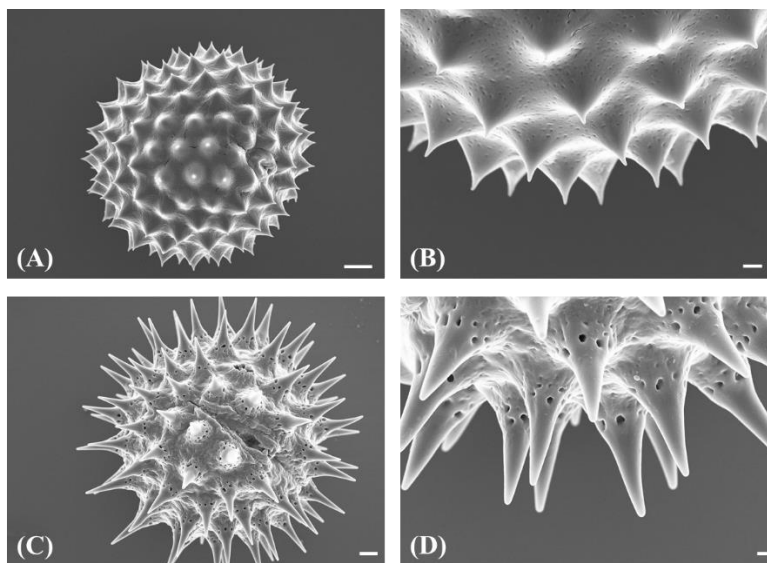


Figure 1. SEM images indicating the surface morphology of pollen grains: ragweed pollen at low (A) and high (B) magnification, and sunflower pollen at low (C) and high (D) magnification. The scale bars are 2 μm for (A) and (C), and 500 nm for (B) and (D).

Results and Discussion

Loading-Dependent Adhesion on Rough Natural and Synthetic Substrates. We observed a strong pressure-sensitive adhesion in Figure 2 between echinate pollen particles (Pr_C and Psf_C) and sunflower stigma surfaces, but not on flat substrates. For example, under loading forces (F_L) up to 500 nN, the adhesion forces (F_{ad}) of Psf_C on Si and PS surfaces are almost constant (~60 nN) and independent of the load applied, suggesting no pressure effect and

no substrate or pollen deformation. In marked contrast, a strong dependence on load F_L was observed for the pollen particles interacting with the stigma surface. The F_{ad} versus F_L curve showed three regimes: below $F_L = 50$ nN the adhesion forces increased slowly from ~90 nN to 100 nN; between $F_L = 50$ and 200 nN F_{ad} increased steeply; and above 200 nN no appreciable increase was observed and F_{ad} reached a plateau around 180 nN.

The increased pull-off adhesion suggests that either the surface area of contact and/or the number of spine contacts with the stigma was increasing with load forces beyond F_L of 50 nN. The sunflower and ragweed pollen spines are roughly arranged at a spacing that is complementary to the size of the receptive papillae on the stigma. This complementarity can explain the observed loading-dependent adhesion, considering that the spines could align with the complementary-patterned surfaces of the papillae, resulting in increased contact area. Once the patterns have aligned, further loading would be unlikely to result in higher adhesion, which is consistent with the plateau at 180 nN.

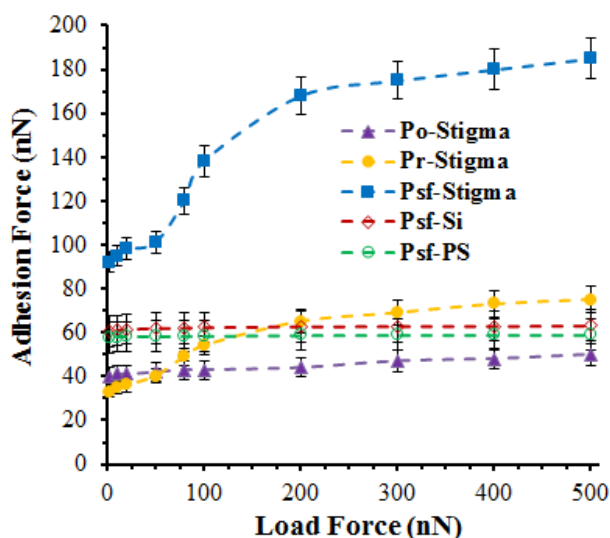


Figure 2. Adhesion force (F_{ad}) versus normal loading force (F_L) for each pollen particle (Po = olive, Pr = ragweed, Psf = sunflower) interacting with different substrates (Stigma = cleaned sunflower stigma, . Error bars are 95% confidence intervals. Reproduced with permission from reference 10.

On the blended PS + PSI surfaces that mimic the undulating patterns on the sunflower stigma (not shown), a similar load-dependent adhesion was also observed, but only on substrates with roughness above a critical value and patterns that matched the spacing of pollen spines. With increasing load forces, the adhesion forces of clean sunflower pollen particles interacting with the two roughest surfaces, PSI2 and PSI3, increased proportionately from ~90 nN to ~160 nN between 2.5 nN and 500 nN load forces. The ragweed adhesion force increased proportionately also on PSI2 and PSI3. However, the adhesion force of clean olive particles with reticulated surface interacting with PSI2 and PSI3 was not significantly changed with the load forces. The load dependence suggests the forced alignment of pollen spikes with the pattern on the rough patterned polymer surface under higher loads.

Hydrodynamic and Capillary Forces and Rate-Dependent Adhesion of Pollen. To provide a pollen-kitt-free control, the “dry” adhesion between ragweed pollen and Si was measured and is presented in Figure 3 (A). The wet adhesion of ragweed pollen on Si mediated by a pollen-kitt liquid bridge is presented in Figure 3 (B). The approach curves for wet adhesion showed much stronger jump-in forces (≈ 450 nN) than for dry adhesion, and the jump-in force occurred at a longer separation distance of ~ 1.8 μm from the Si substrate (Figure 3 (B)). The magnitude and range of wet adhesion became stronger as the speed of retraction increased, eventually doubling in magnitude at the highest rate probed of 67000 nm/s. Retraction curves of dry adhesion were independent of separation rate (Figure 3 (A)). Compared to the previous dry adhesion study of ragweed pollen based on Hamaker equation, the measured dry adhesion in these experiments (40~50 nN) had similar values.⁸

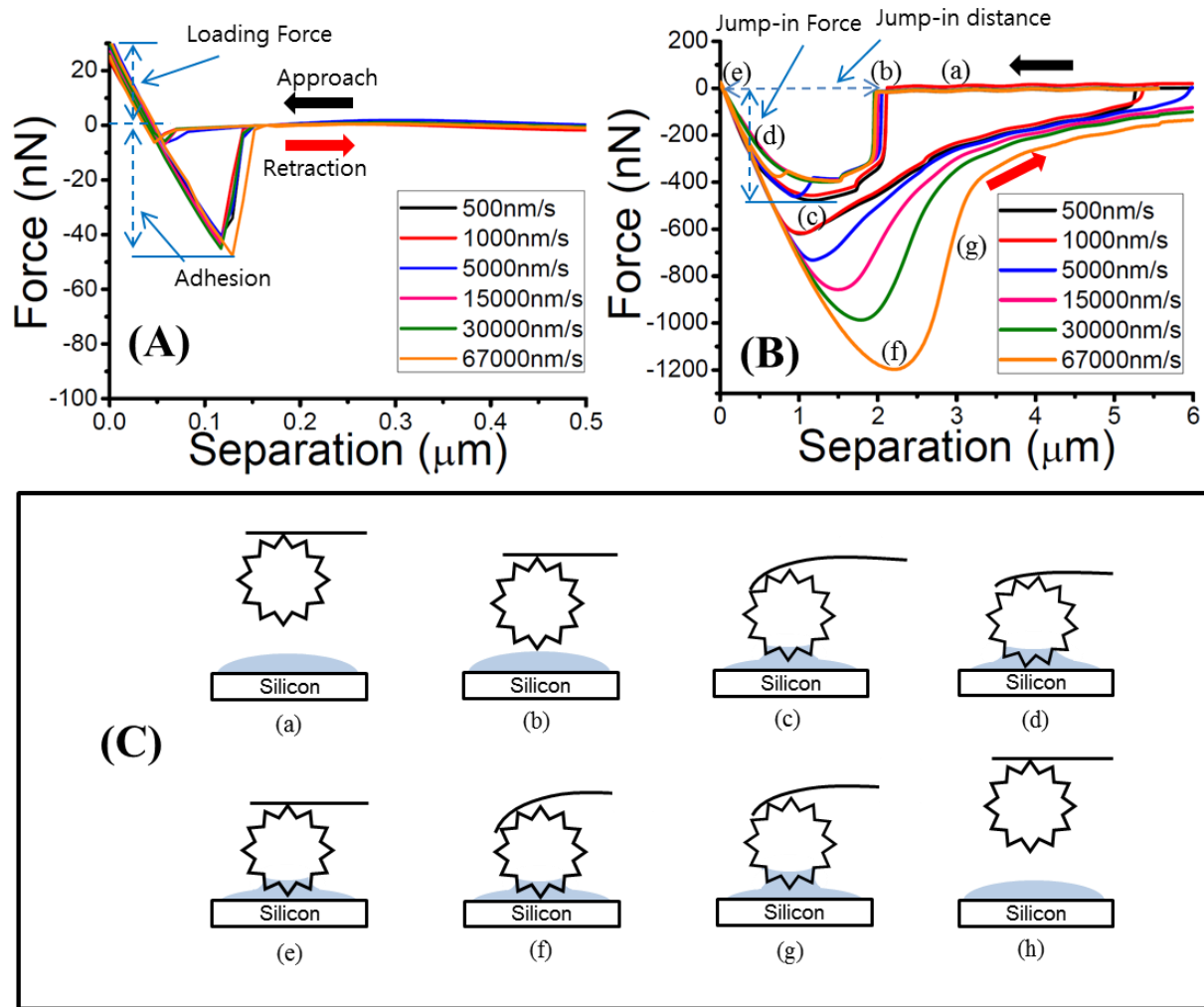


Figure 3. Comparison of AFM force-distance curves at different separation rates from 500 nm/s to 67000 nm/s. (A) Dry adhesion of ragweed pollen on Si substrate. (B) Wet adhesion between ragweed pollen and pollen-kitt film on Si substrate. (C) Schematic of the wet adhesion events ((a) ~ (g) of the curves in (B)) of pollen and pollen-kitt showing the response of cantilever bending.

In contrast, the jump-in force of the wet adhesion was attributed to the capillary forces of the liquid bridge. Figure 3 (C) shows the wet adhesion events and their correlation with cantilever bending. When the pollen particle contacted (Figure 3 (B)) the liquid surface, the pollen experienced both a capillary force toward the pollenkitt film and the elastic force of cantilever toward the other side. The jump-in distance was dependent on the initial thickness of the liquid pollenkitt. The jump-in distance of wet adhesion in this experiment was about 1.8 μm , much longer than for dry adhesion (about 10 nm). The maximum bending of the cantilever by the jump-in force occurred at 1.2 μm above the surface (Figure 3 (c)), and the approaching rate of the particle became slower than the cantilever after the maximum bending point due to the viscous resistance of the liquid (Figure 2 (d)). Finally, the pollen didn't move further after it reached the minimum separation distance from the solid surface (Figure 3 (e)).

The force magnitude and separation rate dependence of the pollen wet adhesion were significantly different from those observed for dry adhesion. It is well known that two forces, the capillary force (F_c) and viscous force (F_v), mainly contribute to the wet adhesion (F_w) between two solid surfaces bridged by a liquid meniscus.¹

$$F_w = F_c + F_v \quad (1)$$

The magnitude of the capillary and viscous forces of ragweed pollen (Figure 3 (B)) can be understood by a wet adhesion model of a spherical particle and a planar surface. Multiple step-like features were not observed in the retraction curves of wet adhesion in Figure 3 (B), indicating that a single liquid bridge is present (as opposed to multiple bridges on individual spines). The SEM image in Figure 1 indicates that the average length of ragweed spines is about 900 nm, about half of the film thickness, allowing the spines to be fully immersed in the pollenkitt film ($\approx 1.8 \mu\text{m}$). Thus, the SEM and force profiles are consistent with formation of a single liquid bridge between the spherical core body of the pollen and the solid substrate, instead of having multiple liquid bridges with each spine.

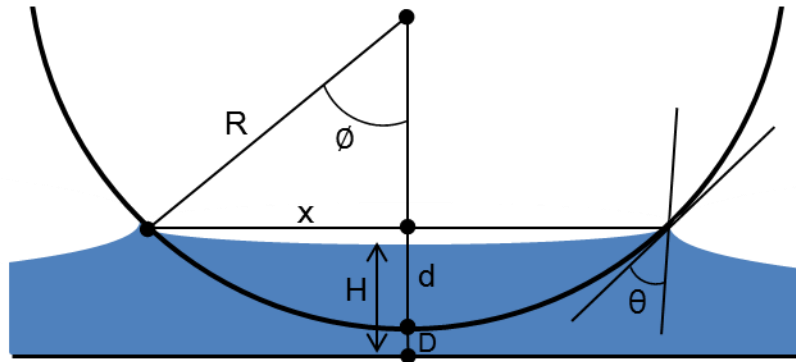


Figure 4. Schematic of a liquid bridge between a sphere and liquid film. This schematic is relevant to cases in which pollen spines are short enough to be fully immersed in the liquid film, allowing wetting of liquid on the core pollen body.

The hydrodynamic response was not observed at retraction rates below 5000 nm/s, and the force magnitude of wet adhesion in this range of separation rates could be explained by the estimated capillary force from a sphere–plane model (Figure 4). The surface tension and Laplace pressure are the two main components of the capillary force.¹¹ The capillary force was quantified

by methods discussed elsewhere¹¹ by assuming that the Laplace pressure difference in the pollenkitt film due to surface forces is negligible, and evaporation and condensation of liquid during the force measurement are also negligible. The capillary force estimation was 690 nN, reasonably close to the actual measured capillary force of 621 nN \pm 13 nN. Both the estimated and measured capillary adhesion forces (Figure 3 (B)) were one order magnitude higher than the dry adhesion forces that are caused by vdW interactions (Figure 3 (A)).

As shown in the retraction curves for wet adhesion in Figure 3 (B), the adhesive forces begin to increase in both magnitude and range at separation rates above 5000 nm/s. The magnitude and range of wet adhesion eventually doubles at the highest rate probed of 67000 nm/s. An explanation of this dynamic response lies in understanding the combined effects of a static capillary force (independent of separation rate) and a dynamic viscous force (rate dependent). The added adhesive force that appears at rates exceeding 5000 nm/s is attributed to viscous response. The viscous force between a spherical particle and flat plate, moving along a line normal to both surfaces can be approximated by¹²

$$F_v = 6\pi\eta R^2 \left(\frac{1}{D}\right) \frac{dD}{dt} \quad (2)$$

which has the form of Stokes drag on a sphere $[(6\pi\eta R) \times \text{velocity}]$ amplified by a geometric factor (R/D) , where the η is the viscosity of the liquid. A dependence of adhesive force on separation rate is described by equation (2), and while this viscous term is expected to dominate the behavior of highly viscous liquids, it can also become very important for liquids of modest viscosity at high shear rate. The rate-dependent adhesive forces, which appear only at a rate of 5000 nm/s and higher, suggest that the magnitude of the viscous force becomes comparable to the static capillary forces only above this separation rate. The viscosity of pollenkitt was measured by a cone and plate viscometer (data not shown). By using this approach, the magnitude of the viscous forces between pollen and pollenkitt were successfully modeled. The contribution of viscous forces to total adhesion is $< 6.3 \%$ of the total force at separation rates below a critical value (5000 nm/s). However, the viscous forces become comparable to the capillary force near this critical value, and dominate at higher separation rates.

Conclusion

Here, we report the first observation of pattern-mediated pressure-sensitive adhesion of a microparticle, by observing the adhesive forces of sunflower pollens on native sunflower stigma surfaces. Evidence suggests that the strong pressure-sensitive adhesion arises from the interlocking of complementary-sized patterns of the pollen spines and stigma surfaces. Inspired by the stigma surface, a series of tunably-patterned polymer surfaces were fabricated by the phase-separation of blends of PS with PSI, which enabled mimicry of the pressure-sensitive adhesion. The wet adhesion of a pollen and pollenkitt has an unusual strong dynamic response (viscous force) at low separation rates (> 5000 nm/s) compared with other rate-dependent adhesives in Nature, such as residues on spider webs⁶, gecko setae³⁶, and ant pads.³⁷ This special feature is due to the relatively high viscosity (above 1 Pa·s) at low shear rate (shear thinning below 20 s^{-1}) of pollenkitt. The contribution of viscous force to wet adhesion was increased exponentially at the low separation rate as long as the separation rate increased, and the viscous force became comparable to the capillary force at the separation rate above the 5000 nm/s. The

size and shape of the pollen surface feature immersed in the liquid tunes the magnitude and sensitivity of hydrodynamic response.

Acknowledgement. Acknowledgment is made to AFOSR grant number FA955010-1-0555 for financial support.

References

1. Cai, S.; Bhushan, B. Meniscus and Viscous Forces during Normal Separation of Liquid-Mediated Contacts. *Nanotechnology*, **2007**, *18* (46), 465704.
2. Pacini, E.; Hesse, M. Pollenkitt – Its Composition, Forms and Functions. *Flora - Morphol. Distrib. Funct. Ecol. Plants*, **2005**, *200* (5), 399–415.
3. Sahni, V.; Blackledge, T. a; Dhinojwala, A. Viscoelastic Solids Explain Spider Web Stickiness. *Nat. Commun.*, **2010**, *1* (2), 19.
4. Eisner, T.; Aneshansley, D. J. Defense by Foot Adhesion in a Beetle (Hemisphaerota Cyanea). *Proc. Natl. Acad. Sci.*, **2000**, *97* (12), 6568–6573.
5. Persson, B. N. J. Wet Adhesion with Application to Tree Frog Adhesive Toe Pads and Tires. *J. Phys. Condens. Matter*, **2007**, *19* (37), 376110.
6. Huber, G.; Mantz, H.; Spolenak, R.; Mecke, K.; Jacobs, K.; Gorb, S. N.; Arzt, E. Evidence for Capillarity Contributions to Gecko Adhesion from Single Spatula Nanomechanical Measurements. *Proc. Natl. Acad. Sci., U. S. A.*, **2005**, *102* (45), 16293–16296.
7. Edlund, A. F.; Swanson, R.; Preuss, D. *Plant Cell*, **2004**, *16*, S84.
8. Lin, H.; Gomez, I.; Meredith, J. C. *Langmuir*, **2013**, *29*, 3012.
9. Lin, H.; Lizarraga, L.; Bottomley, L. a; Carson Meredith, J. Effect of Water Absorption on Pollen Adhesion. *J. Colloid Interface Sci.*, **2015**, *442*, 133–139.
10. H. Lin and J. C. Meredith, “Pressure- and Pattern-Sensitive Adhesion and Detachment of Pollen on Surfaces,” *Soft Matter*, **2016**, in press.
11. Butt, H.-J.; Kappl, M. Normal Capillary Forces. *Adv. Colloid Interface Sci.*, **2009**, *146* (1-2), 48–60.
12. Chan, D. Y. C.; Horn, R. G. The Drainage of Thin Liquid Films between Solid Surfaces. *J. Chem. Phys.*, **1985**, *83* (10), 5311.